

AD-A190 094

EFFECTS OF COPPER AND PHOSPHORUS IMPURITY CONTENT AND

1/1

THERMAL AGEING ON T. (U) ATOMIC ENERGY RESEARCH

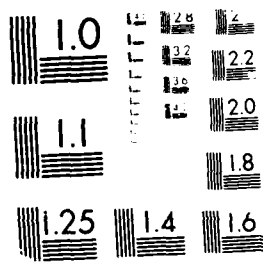
ESTABLISHMENT HARWELL (ENGLAND) S G DRUCE ET AL.

UNCLASSIFIED

DEC 86 AERE-R-11815

F/G 11/6.1 NL

END



MICROCOPY RESOLUTION TEST CHART  
 1010A

3 DOCUMENT IS INTENDED FOR PUBLICATION IN THE OPEN LITERATURE.  
If it is published, it may not be circulated, or referred to outside the organisation to  
which copies have been sent.

①

AD-A190 094

United Kingdom Atomic Energy Authority

**HARWELL**

DTIC  
ELECTE  
S JAN 11 1988 D  
~D

**Effects of copper and phosphorus  
impurity content and thermal ageing  
on the corrosion fatigue behaviour  
of A533B pressure vessel steel**

S G Druce and G Shrimpton

DISTRIBUTION STATEMENT  
Approved for public release  
Distribution Unlimited

COPYRIGHT AND REPRODUCTION  
Enquiries about copyright and reproduction should be addressed to the  
Publications Office, AERE Harwell, Oxfordshire, England OX11 0RA.

Materials Physics and Metallurgy Division  
Harwell Laboratory, Oxfordshire OX11 0RA

December 1986

APPROVED FOR PUBLICATION

C14

87 12 83 282

## ABSTRACT

Materials Physics and Metallurgy Division  
Harwell Laboratory

December 1986 .

HL86/1477 (C14)

(i)



A-1

## CONTENTS

	<u>Page No.</u>
1. Introduction	1
2. Experimental Details	2
2.1 Materials and heat treatments	2
2.2 Fatigue testing	2
3. Results	4
3.1 Crack growth data	4
3.2 Fractography	5
4. Discussion	6
Conclusions	10
Acknowledgements	11
References	12

## TABLES

### Table

1	Chemical Analyses of Experimental Melts of MnMoNi Steels	13
2	Typical Water Conditions	14

#### ILLUSTRATIONS

- Figure 1    Fatigue crack growth data for 'pure' cast of MnMoNi steel.
- Figure 2    Fatigue crack growth data for copper doped MnMoNi steel.
- Figure 3    Fatigue crack growth data for phosphorus doped MnMoNi steel.
- Figure 4    Environmental enhancement of fatigue crack growth.
- Figure 5    Fracture appearance of quenched and tempered 'pure' MnMoNi steel tested in vacuum.
- Figure 6    Fracture appearance of quenched, tempered and aged phosphorus doped MnMoNi steel tested in vacuum.
- Figure 7    Fracture appearance of quenched and tempered 'pure' MnMoNi steel tested in high purity, low oxygen water.
- Figure 8    Fracture appearance of quenched and tempered copper doped MnMoNi steel tested in high purity, low oxygen water.
- Figure 9    Fracture appearance of quenched and tempered phosphorus doped MnMoNi steel tested in high purity, low oxygen water.
- Figure 10   Fracture appearance of quenched, tempered and aged phosphorus doped MnMoNi steel tested in high purity, low oxygen water.

## 1. Introduction

Mechanically dominated fatigue crack growth at stress intensities intermediate between threshold and unstable fracture is generally considered to be insensitive to material composition and microstructure. Ferritic, bainitic, pearlitic and martensitic steels all exhibit similar growth rate kinetics when plotted on logarithmic axes of growth rate per cycle ( $da/dn$ ) and alternating stress intensity range ( $\Delta K$ ), and show little sensitivity to changes in load ratio ( $R=K_{min}/K_{max}$ ), cyclic frequency or waveform.

Environmentally assisted fatigue may result in a change in crack growth mechanism, and hence affect the growth kinetics, through a variety of phenomena arising from the chemical activity at the crack tip. In aqueous environments exposure of clean metal surfaces during cyclic loading leads to the anodic dissolution of iron, with the corresponding cathodic reaction of oxygen reduction or hydrogen evolution. Crack advance arising from purely mechanical damage can be enhanced by two mechanisms: electrochemical removal of material at the crack tip per se, that is, anodic dissolution, or hydrogen assisted cracking processes in the immediate crack tip vicinity. These mechanisms are sensitive to material parameters and therefore under conditions promoting environmentally assisted fatigue there is potential for both mechanical loading factors and material variables to control growth kinetics. For example, anodic dissolution might be expected to be increased by compositions and heat treatments leading to local galvanic cells or low re-passivation rates, whereas hydrogen assisted cracking would be enhanced by treatments resulting in an increased hydrogen source:sink ratio. Both environmental mechanisms are potentially affected by changes in grain boundary chemistry, and several workers<sup>(1-3)</sup> have shown that hydrogen embrittlement during static loading is exacerbated by grain boundary impurity segregation. Loading parameters such as stress range, stress ratio and cyclic frequency will control the dislocation activity at the crack tip and therefore also potentially affect the rate of crack-tip corrosion.

The objectives of the present study are to investigate the sensitivity of fatigue crack growth kinetics to the presence of two common steel impurity elements in the presence of high purity water at 50°C, and to identify the changes in growth mechanisms giving rise to changes in growth rate behaviour. Results are presented for three experimental melts of a 1.5%Mn 0.5%Mo 0.3%Ni low alloy steel: a high purity melt, and casts individually doped with copper and

phosphorus. Each composition has been examined in two heat treatment conditions: quenched and tempered, with and without an additional thermal ageing treatment to induce grain boundary segregation. Fracture modes have been assessed by post test analysis in the scanning electron microscope and the results are discussed with reference to published data obtained in water and gaseous hydrogen environments.

## 2. Experimental Details

### 2.1 Materials and heat treatments

The three experimental casts were produced with a nominal ASTM A533B alloying element composition by vacuum melting high purity Japanese electrolytic iron with pure alloying additions. A533B and similar MnMoNi steels are used extensively in the fabrication of Pressurised Water Reactor (PWR) pressure vessels. The 'pure' cast contains concentrations of the impurity elements sulphur, phosphorus and copper typical of modern good quality commercial steels. The levels of phosphorus and copper in the respective doped casts (i.e. 0.45% and 0.4%) are in excess of the maximum permitted by commercial specifications. Full chemical analyses are given in Table 1.

Following casting, the 125mm square section ingots were hot forged into bars approximately 70mmx30mm. Sections of the bar were given a homogenising heat treatment at 1100°C for 50h to reduce chemical inhomogeneity arising from solidification segregation. Specimen blanks were then austenitised at 1100°C for 1hr, water quenched and tempered at 650°C for 1hr, followed by water quenching to minimise grain boundary segregation of impurities during cooling. 25mm thick compact specimens were then machined from the blanks. Half the specimens were given an ageing treatment of 1000h at 500°C under vacuum, followed by a slow cool. The resultant prior austenite grain sizes as measured by linear intercepts from optical micrographs were 99µm for the pure cast and 154µm and 104µm for the copper and phosphorus doped casts respectively.

### 2.2 Fatigue testing

Constant load amplitude crack growth tests were performed in high purity low oxygen water for each of the three material compositions in the two heat treatment conditions. A sinusoidal waveform of frequency 0.1Hz and stress ratio ( $P_{min}/P_{max}$ )-0.2 was used for these tests. The initial  $\Delta K$  at the start of test following precracking was generally in the range 12-15 MPa/m. Precracking was performed in the test environment at a higher frequency,



typically 1Hz, ensuring that  $K_{max}$  at no time exceeded the start-of-test value. Crack length was monitored using a microprocessor based direct-current potential-drop technique giving a short-term crack extension resolution of 0.02mm and long-term stability of 0.2mm. Growth rates were calculated from the measurements of crack length and number of cycles by polynomial fitting in accordance with ASTM E647. Details of the crack monitoring equipment and data analysis procedures are given elsewhere<sup>(4,5)</sup>. Specimens were horizontally supported in environmental chambers, with the water level set to the loading line. The chambers, together with the specimen grips, loop pipework, pump, holding tank and heat exchangers, were all constructed from stainless steel. During testing, argon gas was continuously bubbled through the holding tank at a rate of 1 litre/min and provided a cover gas in the environmental chamber. The resultant oxygen content of water sampled from close to the specimen and measured using an 'Orbisphere' analyser was typically 4ppb. Water flow through the chamber was 2 litre/min, giving an equivalent volume change every 8 minutes. In addition to flowing through the chamber and back to the holding tank, water was continuously pumped from the holding tank through a mixed anion/cation exchange resin at a flow rate of 2 litre/min. The resultant conductivity was 0.04-0.06  $\mu S/cm$ . Water samples were drawn off at intervals for analysis of anion concentration. Typical water conditions and impurity levels are given in Table 2. Test temperature was controlled at  $50 \pm 1^\circ C$  by heating the feedwater to the chamber and thermally insulating all external surfaces. A conditioning period of 2 days was allowed prior to precracking to promote equilibrium conditions prior to testing. The total duration of each test was typically 2-3 months.

In addition to aqueous environmental testing, high vacuum ( $2 \times 10^{-4} Pa$ ) fatigue tests have been performed using the pure cast material in the quenched, and tempered condition and the phosphorus doped material in the quenched, tempered and aged condition. The test frequency was 1Hz with an R ratio of 0.2 and test temperature of  $40 \pm 2^\circ C$ . The data from these tests were used as a baseline for evaluation of the environmental component of growth in water.

On completion of testing all specimens were broken open in liquid nitrogen and the surface oxide removed in a proprietary solution in preparation for examination optically and in the scanning electron microscope.

### 3. Results

#### 3.1 Crack growth data

Figure 1 shows crack growth data for the 'pure' material conventionally expressed on logarithmic axes of growth rate,  $da/dn$  and stress intensity range,  $\Delta K$ . Also shown are the ASME 1983 Boiler and Pressure Vessel Code reference growth curves commonly used for the fatigue evaluation of subsurface (dry) and surface breaking (wet) defects in the reactor pressure vessel of the PWR. These are included for comparison and to provide a common reference for subsequent figures. The data from the vacuum test is linear with a slope of approximately 5 and lies consistently beneath the the ASME 'Dry' line by a factor of 10 at low stress intensities, decreasing to a factor of 2 at high stress intensities. The data from water tests on aged and unaged material exhibit 'hooked' shaped curves with enhanced growth rates when compared with the vacuum data, but do not exceed the ASME 'Wet' line. The effect of the ageing heat treatment appears to increase marginally the growth rate at  $\Delta K$  values less than 35 MPa/m.

Figures 2 and 3 show growth rate data for the copper doped and phosphorus doped materials. The vacuum line refers to the pure cast data shown in Figure 1. The vacuum data for the quenched, tempered and aged phosphorus doped material (Figure 3) agree closely with the quenched and tempered pure cast. Tests in the water environment show both copper and phosphorus doped materials to exhibit the same general hook shaped growth curve as found in the pure cast, and generally higher growth rates in the aged condition. Additional features shown in the water for the phosphorus doped material only are: (i) an initial deceleration in growth rate with increasing  $\Delta K$  at the beginning of the tests; (ii) erratic transient high growth rates in the aged condition at  $\Delta K$  values in excess of 40 MPa/m. The initial deceleration in the aged material occurred over a total crack extension of 3mm lasting some  $10^5$  cycles, that is 11 days of testing, and is not considered to be an artefact of the crack monitoring equipment.

Figure 4 shows the growth rate data expressed in terms of the degree of environmental enhancement referenced to the data from the pure cast material obtained under vacuum. All materials in the quenched and tempered condition exhibit environmentally enhanced growth in the  $\Delta K$  range 20-40 MPa/m peaking at a  $\Delta K=30-32$  MPa/m for phosphorus and copper doped materials with a tenfold enhancement in growth rate. The peak in the pure cast occurs at a lower stress intensity, approximately 25 MPa/m, and the maximum enhancement is greater. The

maximum degree of environmental enhancement increases on ageing in all compositions, being typically 25 times the growth rate in vacuum. The  $\Delta K$  for maximum enhancement is lower in the aged condition than for the quenched and tempered condition for copper doped and phosphorus doped materials, but is the same for the pure cast. Interestingly, comparison of Figures 1-3 with Figure 4 shows that for each test the maximum environmental enhancement has occurred at the same growth rate, i.e.  $5 \times 10^{-7}$  m/cycle independent of the  $\Delta K$  required to produce the growth rate, material composition or heat treatment. Characteristics specific to the aged phosphorus doped material are the maintenance of peak environmental enhancement at low levels of  $\Delta K$ , and the presence of a secondary peak over the  $\Delta K$  range 40-50 MPa/m. For this material and heat treatment unstable fracture occurred at  $\Delta K = 55$  MPa/m.

### 3.2 Fractography

Figures 5 and 6 show the fracture appearance of the 'pure' and phosphorus doped materials when tested in a vacuum. In both cases failure is entirely transgranular and ductile, comprising interconnecting tear ridges. There is little evidence of individual grains influencing the fracture path. Some secondary cracking occurs throughout the entire  $\Delta K$  range and a small amount of microvoiding is observed at high stress intensities. Fatigue striations were not visible at low stress intensities, and only poorly defined at high values when viewed at magnifications up to  $\times 10,000$ . These features are typical of mechanically controlled fatigue in steels.

Figure 7 shows the fracture appearance of the pure material in the quenched and tempered condition when tested in water. At low stress intensities ( $\Delta K=20$  and  $25$  MPa/m), there is a component of smooth intergranular fracture, with the remaining area occupied by ductile transgranular failure, the latter exhibiting a tendency to change plane locally on a scale consistent with the prior austenite grain size. Such an appearance will be referred to as grain orientation control (GOC). Intergranular facets and GOC are not evident at higher stress intensities, where the fracture appearance is similar to that observed from the vacuum test, but with less secondary cracking. Examination of the fracture surface of the pure cast material in the aged condition and tested in water revealed similar features to those from the quenched and tempered condition.

Figure 8 shows the fracture surface of the quenched and tempered copper doped material. At low and intermediate stress intensities there is pronounced GOC of the transgranular failure and a small number of smooth intergranular facets. A distinctive feature of the transgranular fracture is the ridged appearance, which contrary to normal fatigue striations, lie parallel to the macroscopic growth direction. Subsequent metallographic examination of polished and etched specimens, prepared by removing a minimum of material from the fracture surface, suggests that these ridges lie parallel to the tempered martensitic lath structure with each ridge comprising several individual laths. As  $\Delta K$  increases, GOC becomes less pronounced and finally disappears at high stress intensities. Similar features and trends with  $\Delta K$  were observed for the aged condition.

Figures 9 and 10 show the fracture appearance of the phosphorus doped material in the quenched and tempered, and aged conditions respectively. In the quenched and tempered condition the appearance is similar to that observed in the pure cast. Ageing results in a markedly increased proportion of intergranular fracture. At low stress intensities ( $\approx 20 \text{ MPa}\sqrt{\text{m}}$ ) their distribution is fairly random. Above  $25 \text{ MPa}\sqrt{\text{m}}$  the intergranular fracture tends to occur in packets of several grains interconnected by regions of wholly transgranular failure. The packets become larger with increasing  $\Delta K$  and can occupy up to half the total crack front across the specimen, resulting in erratic high growth rates. The appearance of the final unstable fracture region was almost entirely intergranular, with occasional interconnecting ductile ligaments.

#### 4. Discussion

Environmentally enhanced crack growth has been demonstrated for all three compositions in both heat treatment conditions, giving rise to the characteristic 'hook' shaped growth curve<sup>(6)</sup>. The degree of enhancement is affected by heat treatment, generally increasing with ageing at  $500^\circ\text{C}$ . Comparison of water and vacuum test data shows that at  $\Delta K$  levels where growth rate enhancement occurs there are associated changes in fracture morphology, namely:

- i) a reduction in the degree of secondary cracking;
- ii) introduction of GOC transgranular cracking;
- iii) introduction of smooth intergranular cracking.

These observations confirm the presence of a microstructural/environmental

interaction, although it should be noted that the magnitude of the changes in growth rate between materials of differing composition or heat treatment is only modest.

A detailed fractographic examination<sup>(7)</sup> of 44 A533B test specimens tested mainly in high temperature (288°C) water environments has also shown that environmental enhancement was, without exception, accompanied by a change in fracture morphology. The fracture appearance became more brittle, exhibiting regular shallow striations, little secondary cracking, tear ridges in the direction of crack propagation and fan-shaped facets, generally associated with MnS inclusions. When tested at room temperature some intergranular fracture also occurred, but growth rates were largely unaltered. However, contrary to reference 7, the fractographic observations reported here cannot be quantitatively related to the degree of growth enhancement. For example, Figure 4 indicates that environmental enhancement of the copper doped material in the quenched and tempered condition does not rapidly increase until a  $\Delta K$  of 25 MPa/m is attained, whereas Figure 8 shows well developed GOC at 20 MPa/m. Furthermore, ageing promoted the growth rate enhancement, but there was no associated increase in GOC or other environmentally sensitive fracture modes.

Although sensitive to heat treatment, it may be noted that the maximum growth rate enhancement is similar (i.e. x25-30) in all three casts, independent of impurity content. Furthermore, maximum enhancement occurred at a specific growth rate ( $5 \times 10^{-7}$  m/cycle) independent of  $\Delta K$ , material composition and heat treatment. These observations suggest that it is the rate of creation of clean metal surfaces at the crack tip that determines when, i.e. at what  $\Delta K$ , frequency and stress ratio environmental enhancement will occur, and that metallurgical variables control the degree of enhancement. It is suggested that at low growth rates there is insufficient clean metal surface exposed for the associated crack tip chemical activity to enhance growth, and at high growth rates the process is dominated by growth from mechanical fatigue. In these regions there is therefore little or no detectable enhancement. At intermediate growth rates there is a regime where sufficient crack tip chemical activity occurs to produce significant enhancement, compared with the mechanical controlled growth.

Variation in the metallurgical variables reported here, that is copper and phosphorus impurity content and isothermal ageing, have generally resulted in

rather modest changes in growth rate or enhancement, i.e. within a factor of 2-3. Ageing increased growth rates in all three compositions. Previous work<sup>(8)</sup> conducted using the same materials has shown that ageing at 500°C induces temper embrittlement arising from grain boundary segregation of phosphorus. Accordingly, the 'pure' and copper doped materials exhibited relatively small (i.e. about 30°C) increases in the ductile to brittle transition temperature recorded from Charpy impact tests, whereas the phosphorus doped material produced an embrittlement of 150°C. Phosphorus segregation in the phosphorus doped material appears to have had two distinct influences on the fatigue properties in the water environment, depending on  $\Delta K$  range. Firstly, at low  $\Delta K$  values, i.e.  $< 22 \text{ MPa}/\text{m}$  maximum environmental enhancement is maintained, whereas in the other composition and heat treatment conditions the enhancement factor decreases. In this regime randomly distributed intergranular facets augment the fatigue process. Secondly, at higher  $\Delta K$  values, i.e.  $> 40 \text{ MPa}/\text{m}$  approaching the static load toughness, bursts of intergranular fracture occur across large fractions of the total crack front, giving rise to erratic transient high growth rates. It is significant that despite high levels of phosphorus grain boundary segregation, no intergranular fracture was observed in the vacuum test on the aged phosphorus doped material throughout the entire  $\Delta K$  range evaluated, and the observed growth rates were very similar to the quenched and tempered 'pure' material. Hence segregation appears to affect fatigue properties only in the presence of an active environment. It is interesting to note that although maximum environmental enhancement extends over a wider range of  $\Delta K$ , the degree of maximum enhancement in the aged phosphorus doped material is similar to that found in the other composition materials.

With regard to the mechanism of environmental enhancement, one can speculate from the observed growth rate behaviour, post test fractographic analyses and comparison with the literature, but no direct evaluation has been made. It is common to distinguish between anodic dissolution and hydrogen embrittlement as alternative mechanisms of environmentally assisted cracking, but it should be remembered that they are generally the balancing anodic and cathodic reactions of the same corrosive cell and therefore interdependent. In this work environmental growth rate enhancement has been accompanied by a change in fracture morphology to include varying degrees of intergranular fracture and GOC transgranular fracture. It is thought unlikely that anodic dissolution along selective grain orientations would give the same appearance as the GOC failure observed here, and therefore hydrogen embrittlement is

considered a more likely mechanism. This surmise is supported by the results of Atkinson and Lindley<sup>(8)</sup>. In this work, similar environmental enhancement factors were recorded at  $\Delta K$  values greater than 15-20 MPa $\sqrt{m}$  for a commercial cast of A533B tested in hydrogen gas, together with an associated change in fracture mode from ductile striations to transgranular faceting.

Several workers<sup>(1-3)</sup> have shown that under non-cyclic loading conditions intergranular decohesion in quenched and tempered steels is enhanced by the presence of hydrogen. It has been demonstrated that at a fixed hydrogen fugacity the stress required for decohesion decreases as the grain boundary impurity content increases, and for a given level of segregation the stress needed for cracking decreases as the hydrogen concentration increases<sup>(10)</sup>. These observations are entirely consistent with those reported in this work obtained for cyclic loading conditions, where the phosphorus doped material in the aged condition has been shown to exhibit more intergranular fracture and at lower stress intensities than the other compositions and heat treatment conditions.

Another fracture mode induced in iron and steel by hydrogen under static loading is glide-plane decohesion. This is characterised by cracking on {110} or {112} planes, and occurs in tempered bainitic or martensitic lath structures as well as iron single and polycrystals<sup>(10-12)</sup>. It is thought that it is the result of the collection of hydrogen in heavily dislocated slip bands. Mechanical fatigue crack growth will naturally produce slip bands radiating from the crack tip, ideally positioned to become saturated with hydrogen produced by corrosion. Planar slip will be promoted in the presence of hydrogen, further encouraging the formation of predominant slip bands. It is suggested therefore that there will be a tendency to produce crack growth along slip bands under cyclic loading by a mechanism analogous to glide plane decohesion under static loading. The result will be a fracture path dominated by local grain orientation which, at higher magnification, will reflect individual lath orientations. These are the features ascribed to 90° transgranular failure. The effect of ageing in promoting the degree of environmental enhancement is also consistent with hydrogen enhanced fracture mechanisms. It is known that dislocations and vacancies act as moderately strong hydrogen sinks<sup>(13)</sup>. Ageing will reduce the vacancy concentration left by quenching from the tempering treatment and may also result in some sub structuring of the dislocations, reducing their density. If, as suggested, the hydrogen supply is

controlled by the exposure rate of fresh metal surface during fatigue, and remains unaffected by ageing, then the hydrogen sink:source ratio will be less for materials in the aged condition. Hence the effective hydrogen concentration available for enhancing crack growth will be increased by the ageing heat treatment.

Thus the main fractographic observations associated with the environmentally enhanced fatigue crack growth can be satisfactorily explained on the basis of the known effects of hydrogen on plastic flow and rupture under static loading conditions.

#### Conclusions

1. Three experimental melts of A533B pressure vessel steel containing varying amounts of copper and phosphorus have been fatigue tested in high purity water at 50°C in the quenched and tempered, and quenched, tempered and aged heat treatment conditions. Reference data has also been obtained in vacuum. The log da/dn versus log  $\Delta K$  growth rate curves derived from water tests all exhibit a hooked appearance characteristic of environmentally assisted fatigue.
2. Environmentally enhanced growth is restricted to a limited range of  $\Delta K$  (i.e. 20-45 MPa $\sqrt{m}$ ) for all melts in the quenched and tempered condition and for the high purity and copper doped melts in the aged condition. Peak enhancement is found to occur at a specific growth rate ( $5 \times 10^{-7}$  m/cycle) independent of composition, the  $\Delta K$  required to achieve this growth rate, or the heat treatment condition.
3. The maximum environmental enhancement, with reference to data obtained from the pure cast in a high vacuum environment, is similar in all three casts, being a factor of 25-30. The maximum enhancement factor is generally greater in the aged condition as compared to the quenched and tempered condition. In the aged phosphorus doped material, where ageing is known to promote significant grain boundary segregation, environmentally enhanced crack growth extends to lower values of  $\Delta K$  than found in the other materials/heat treatment conditions.
4. When tested in vacuum the fracture appearance is transgranular and brittle over the entire  $\Delta K$  range with little indication of underlying grain



structure. All tests in water exhibited changes in fracture morphology including varying amounts of intergranular failure and transgranular failure, exhibiting a marked dependence on underlying grain orientation. The stress intensity range over which environmentally enhanced growth was observed approximately corresponds to the range where changes in fracture mode occur.

5. The changes in fracture mode and growth rate are consistent with hydrogen induced cracking mechanisms observed under static loading conditions.

#### Acknowledgements

The authors gratefully acknowledge Dr J A Hudson, Dr P Scott, Dr C Hippsley and Dr J Atkinson (CEGB Leatherhead) for their helpful comments in writing this paper, and Mr C Lane for his experimental assistance. This work was performed as part of the Harwell Underlying Fracture programme.

### References

1. T Inoue, K Yamamoto, M Nagumo, in Hydrogen Effects in Metals. Ed I M Bernstein, A W Thompson, AIME 1981, pp777-784.
2. K Yoshino, C J McMahon. Met Trans 1974 5, pp363-370.
3. J Kameda, N Bandyopadhyay, C J McMahon. Suppl to JIM 21, 1980, pp437-440.
4. G Shrimpton, S G Druce. Program FATEST. A program for logging constant load amplitude fatigue test data. UKAEA Report AERE M3484.
5. G Shrimpton. Program DADNEXP. A program to compute crack growth rates from crack length and number of cycles data recorded during fatigue testing. UKAEA Report AERE M3485.
6. T R Mayer, D M Moon, J D Landes. J Press Vess Tech 1977, pp238-247.
7. Fractographic evaluation of specimens of A533B pressure vessel steels. EPRI Report NP 3483, 1984.
8. S G Druce. Acta Met Vol.34, No.2, pp219-232, 1986.
9. J D Atkinson, T C Lindley. "The effect of hydrogen gas on fatigue crack propagation in A533B steel below 100°C and its relevance to environmentally assisted cracking in aqueous environments." TPRD/L/MT10212/M84. CEEB Leatherhead, 1984.
10. C J McMahon, in Hydrogen Effects in Metals. Ed I M Bernstein, A W Thompson, AIME 1981, pp219-234.
11. S Hinotani, F Terasaki, F Nakasato. Suppl to JIM 21, 1980, pp421-424.
12. T Araki, Y Kikuta. Ibid pp425-428.
3. R Gibala, D S de Miglio in Hydrogen Effects in Metals. Ed I M Bernstein, A W Thompson, AIME 1981, pp113-122.

Table 1. CHEMICAL ANALYSES OF EXPERIMENTAL HELTS OF NiHONI STEELS

	C	Mn	Mo	Si	Cr	P	S	Cu	V	As	Sb	B	Sn	W	Nb	O	H	Al
	%	%	%	%	%	ppm	ppm	%	ppm	ppm	ppm	ppm	ppm	ppm	ppm	ppm	ppm	ppm
Pure	Mean (Standard Deviation)	0.24 (0.107)	1.37 (0.03)	0.51 (0.004)	0.54 (0.007)	0.26 (0.02)	0.27 (0.02)	0.04 (0.02)	<100	<200	<100	<100	<100	<100	<100	<100	<100	<100
Cu doped	Mean (Standard Deviation)	0.27 (0.008)	1.39 (0.02)	0.52 (0.010)	0.55 (0.007)	0.28 (0.02)	0.26 (0.02)	0.40 (0.01)	<100	<200	<100	<100	<100	<100	<100	<100	<100	<100
P doped	Mean (Standard Deviation)	0.26 (0.007)	1.44 (0.03)	0.52 (0.006)	0.54 (0.007)	0.29 (0.04)	0.26 (0.04)	<0.01 (0.01)	<100	<200	<100	<100	<100	<100	<100	<100	<100	<100

Notes

- (i) Mean and Standard Deviation calculated from n analysis uniformly sampling each 100 by ingot where n equals 15, 10, 8 and 10 for Pure, S doped, Cu doped and P doped materials respectively (excepting B and Al).
- (ii) Average of two determinations.

Table 2 - Typical Water Conditions

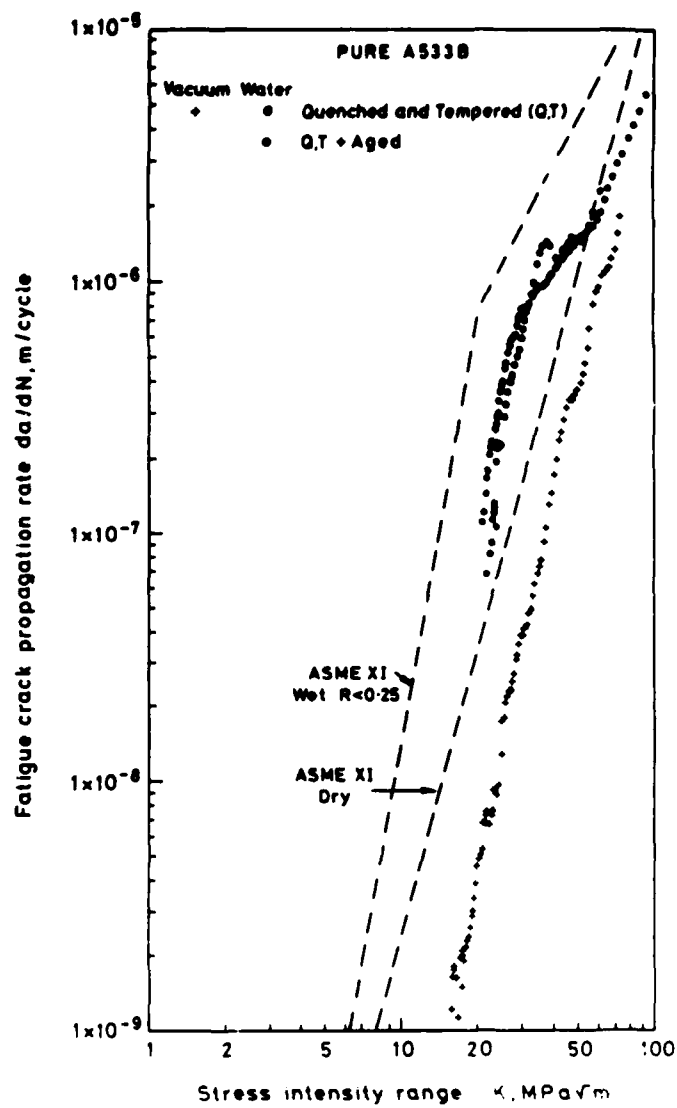
Anion Concentration (ppm)

F <sup>-</sup>	Cl <sup>-</sup>	NO <sup>-</sup>	SO <sub>4</sub> <sup>-1</sup>
0.03	0.06	<0.1	0.05

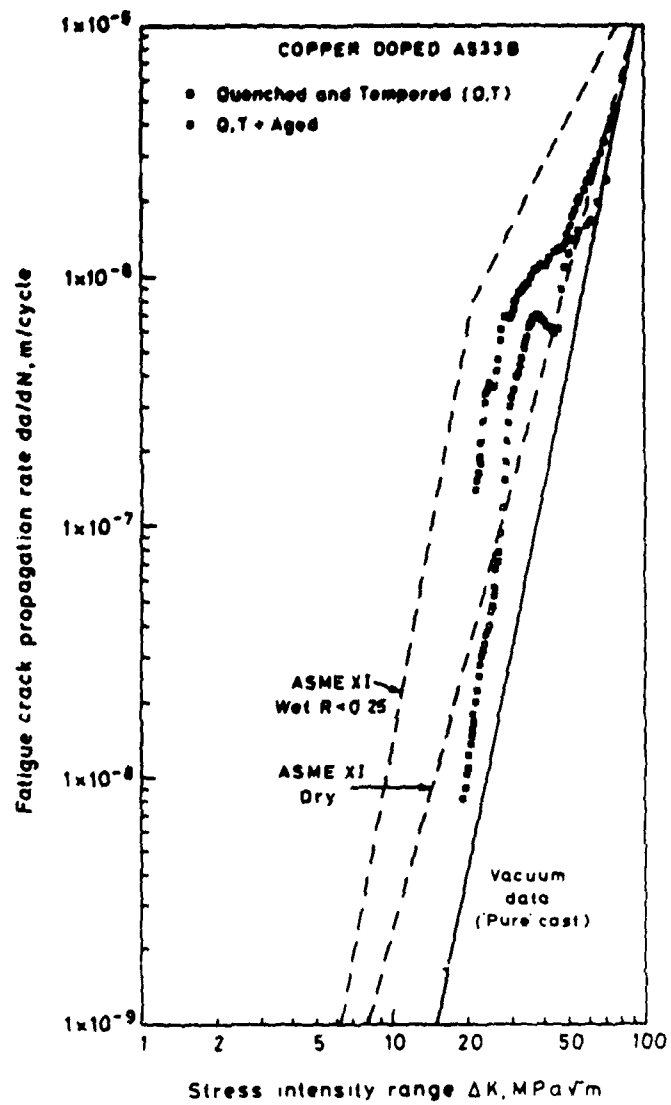
Oxygen concentration

3-6 ppb

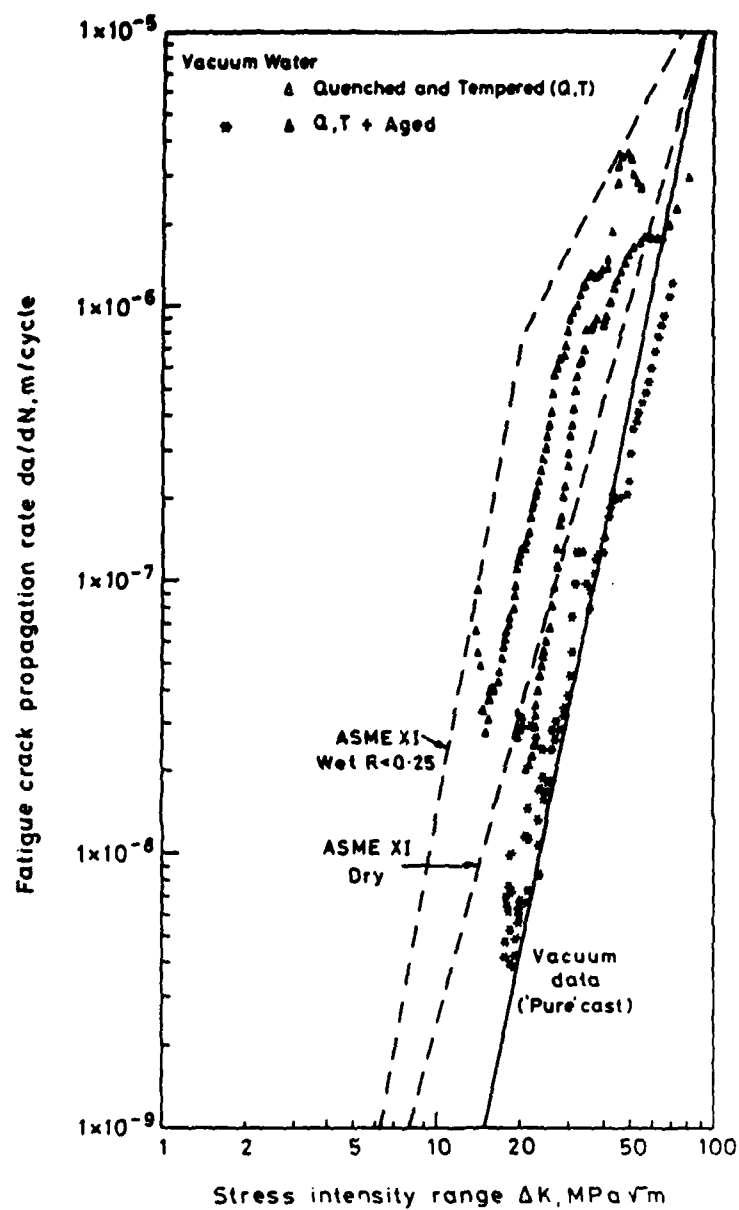
Conductivity 0.04 - 0.06  $\mu$ S/cm



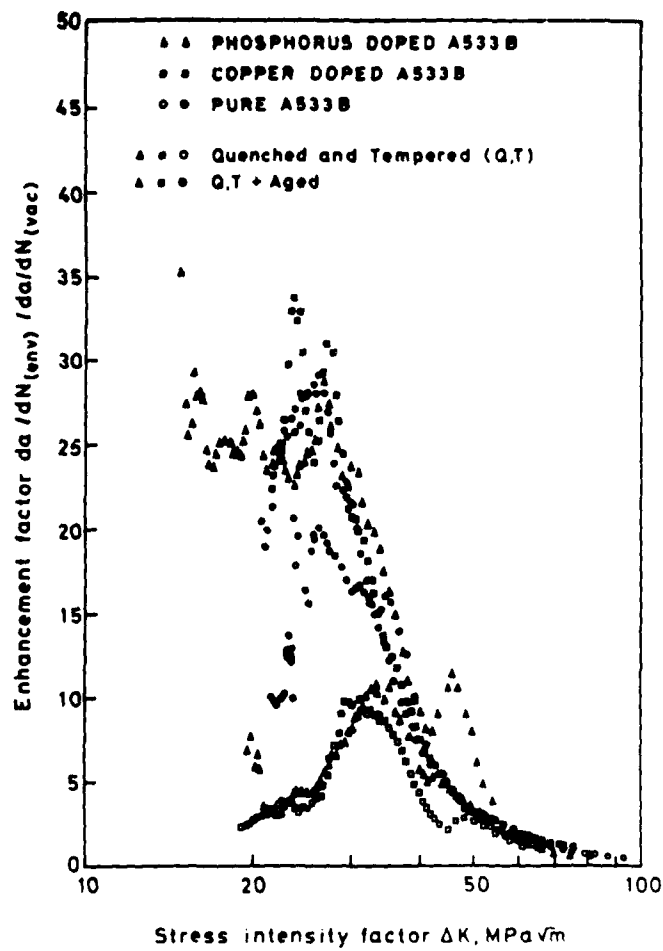
AERE R 11815 Fig. 1  
Fatigue crack growth data for 'pure' cast of 1.25% MoNi steel



AERE R 11815 Fig. 2  
Fatigue crack growth data for copper doped MnMoNi steel



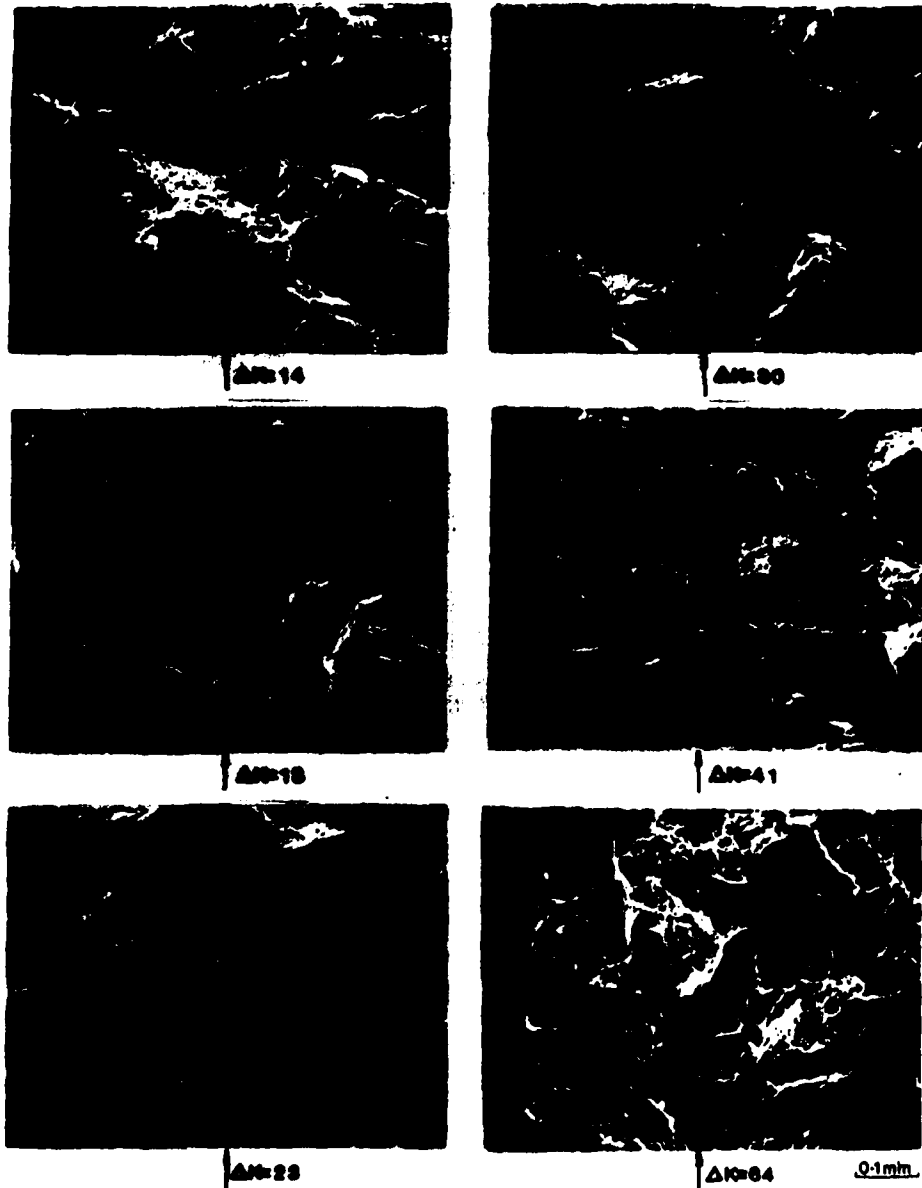
AERE R 11815 Fig. 3  
Fatigue crack growth data for phosphorus doped MnMoNi steel



AERE R 11815 Fig. 4  
Environmental enhancement of fatigue crack growth



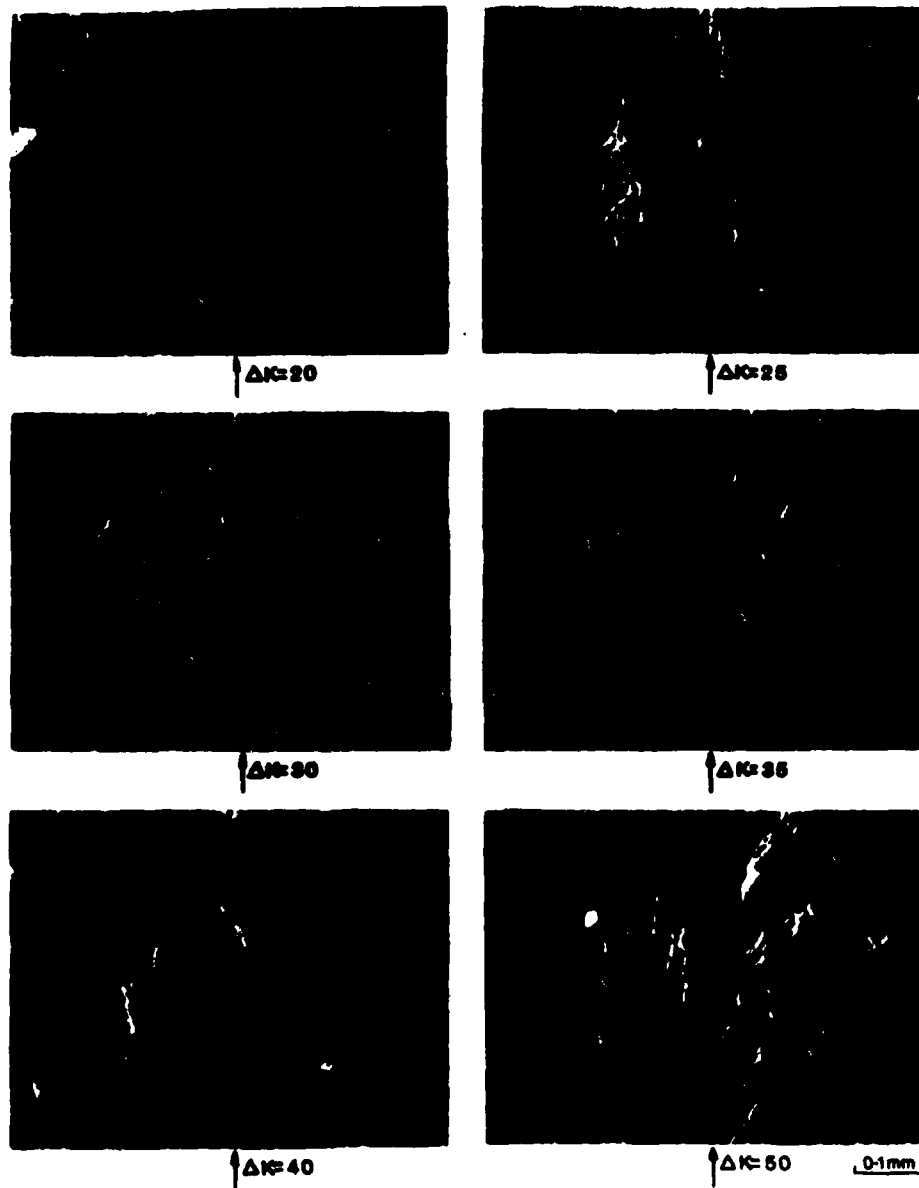
'Pure' Cast (Q-T) Vacuum test



AERE R 11815 Fig. 5  
Fracture appearance of quenched and tempered 'pure' MnMoNi steel tested in vacuum

HARWELL LABORATORY  
PHOTOGRAPHIC GROUP  
HR 24848

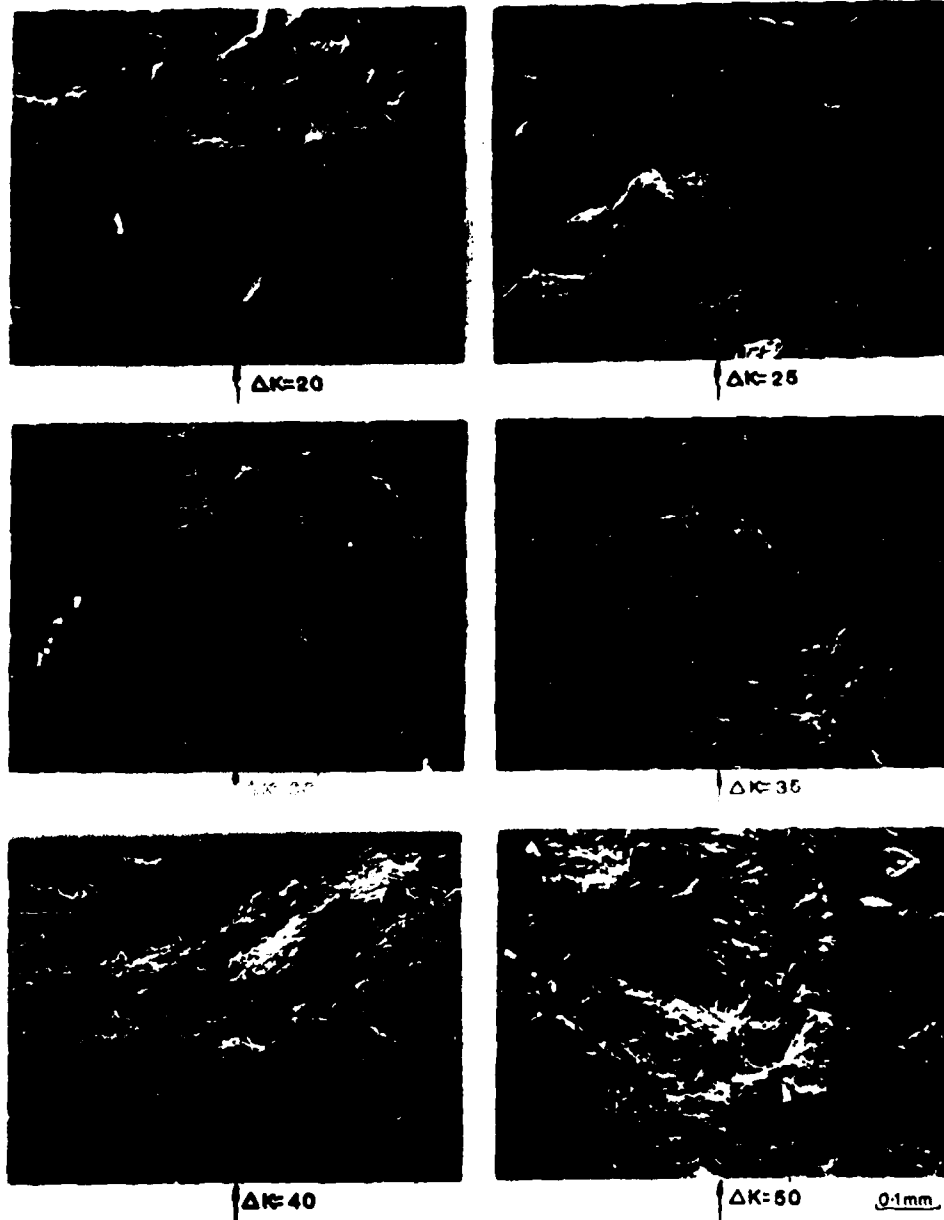
Phosphorus doped (Q-T-E) Vacuum test



AERE R 11815 Fig. 6  
Fracture appearance of quenched, tempered and aged phosphorus doped MnMoNi steel tested in vacuum

HARWELL LABORATORY  
PHOTOGRAPHIC GROUP  
HR 24847

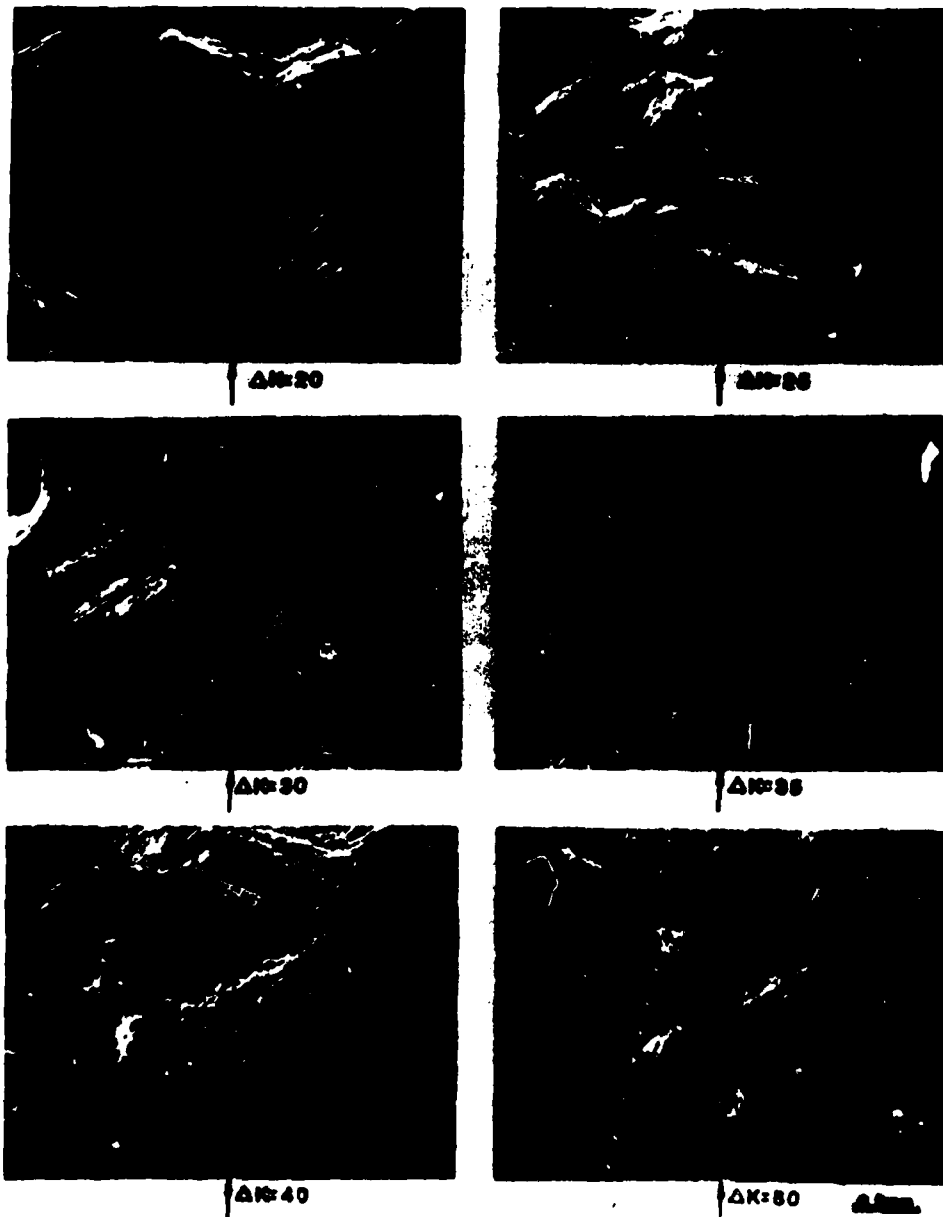
'Pure' Cast (Q+T)



AERE R 11815 Fig. 7  
Fracture appearance of quenched and tempered 'pure' MnMoNi steel tested in high purity low oxygen water

HARWELL LABORATORY  
PHOTOGRAPHIC GROUP  
HR 6655

Copper doped Cast (Q+T)



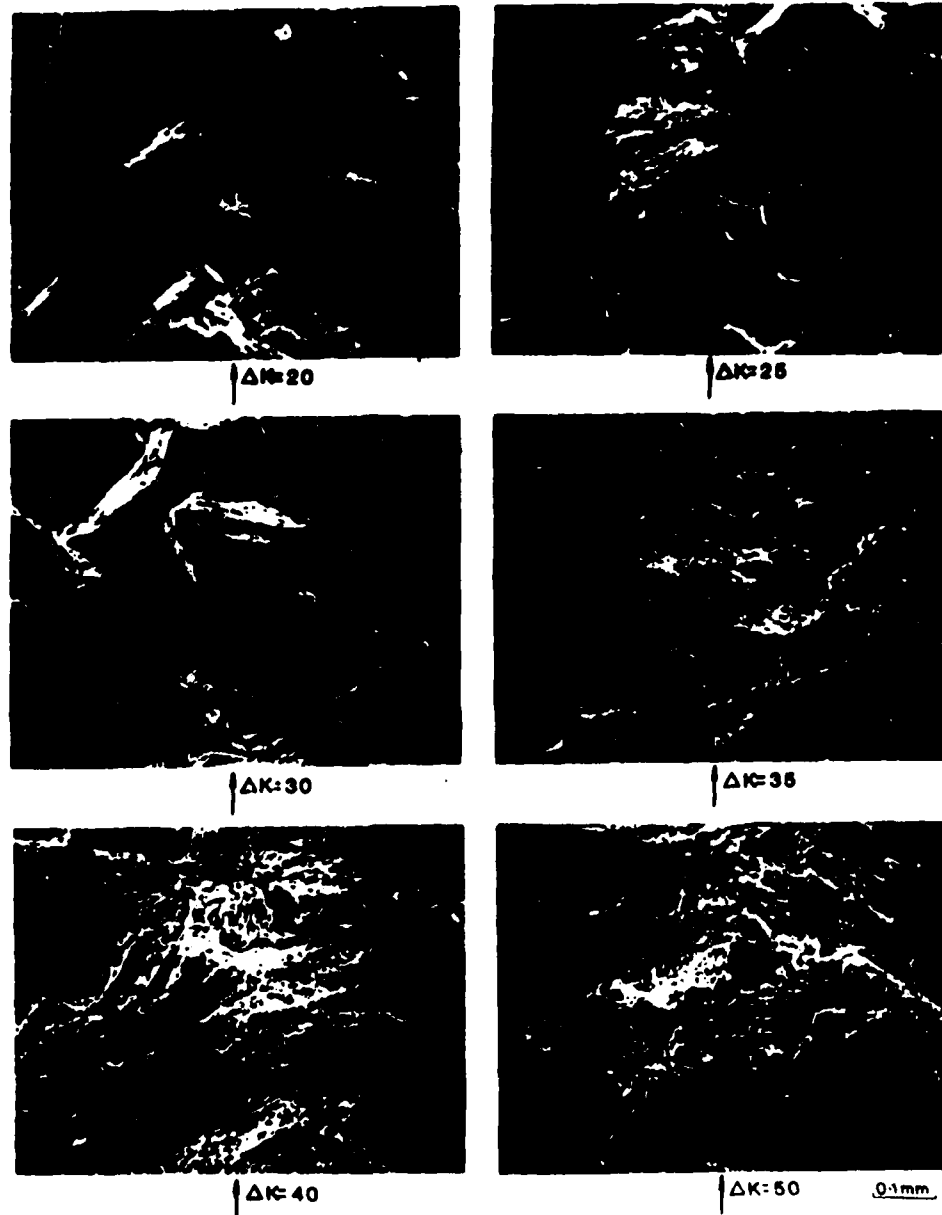
AERE R 11815 Fig. 8

Fracture appearance of quenched and tempered copper doped MnMoNi steel tested in high purity, low oxygen water

HARWELL LABORATORY  
PHOTOGRAPHIC GROUP  
HR 6662



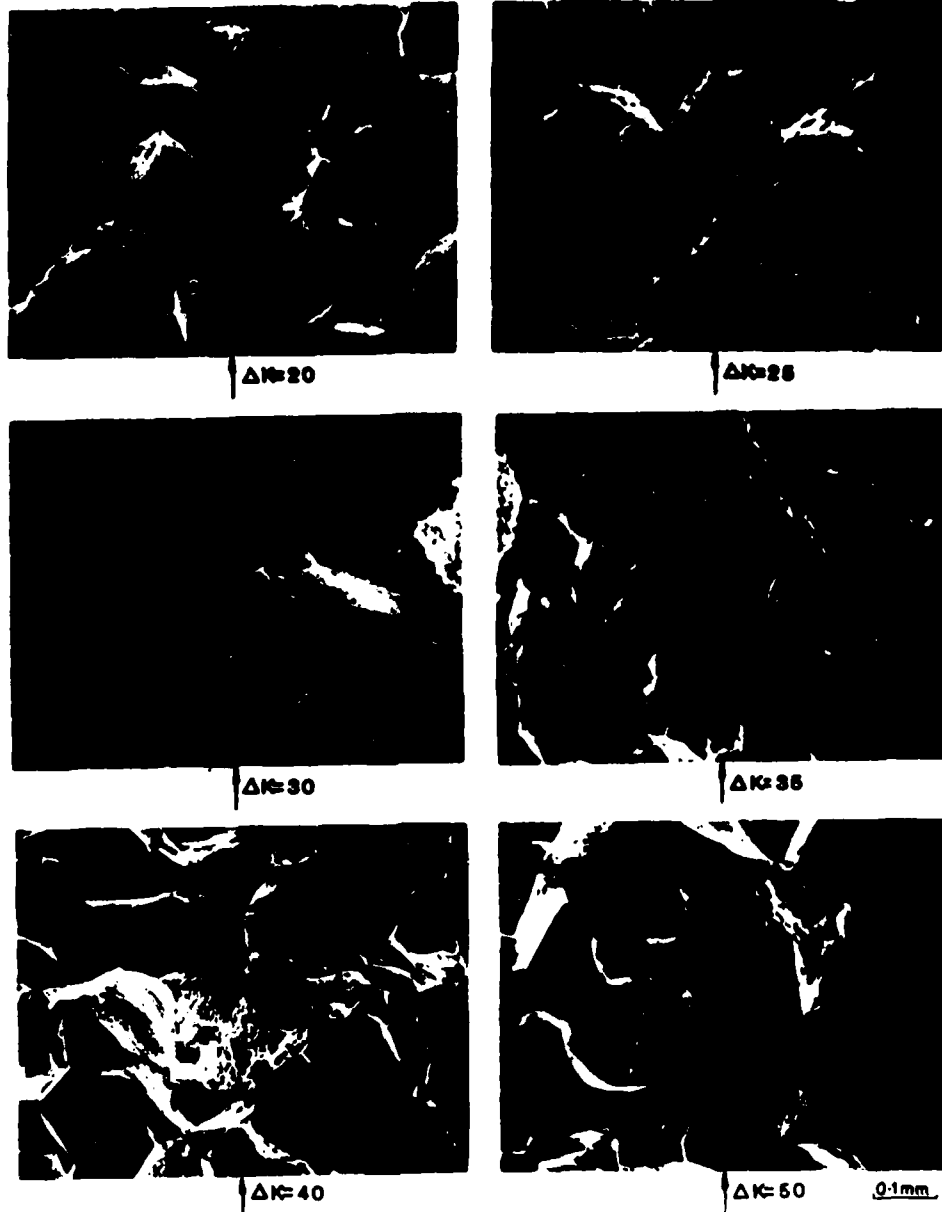
Phosphorus doped Cast (Q+T)



AERE R 11815 Fig. 9  
Fracture appearance of quenched and tempered phosphorus doped MnMoNi steel tested in high purity, low oxygen water

HARWELL LABORATORY  
PHOTOGRAPHIC GROUP  
HR 6714

Phosphorus doped Cast (Q+T+E)



AERE R 11815 Fig. 10  
Fracture appearance of quenched, tempered and aged phosphorus doped MnMoNi steel tested in  
high purity, low oxygen water

HARWELL LABORATORY  
PHOTOGRAPHIC GROUP  
HR 6715

END  
FILMED APRIL 1987

END

DATE

~~FILED~~ FILMED

4 88

DTIC